



HAL
open science

Selective manipulation of microscopic particles with swirling Rayleigh waves

Antoine Riaud, Michael Baudoin, Olivier Bou Matar, Loic Becerra,
Jean-Louis Thomas

► **To cite this version:**

Antoine Riaud, Michael Baudoin, Olivier Bou Matar, Loic Becerra, Jean-Louis Thomas. Selective manipulation of microscopic particles with swirling Rayleigh waves. 2016. hal-01339360

HAL Id: hal-01339360

<https://hal.science/hal-01339360>

Preprint submitted on 29 Jun 2016

HAL is a multi-disciplinary open access archive for the deposit and dissemination of scientific research documents, whether they are published or not. The documents may come from teaching and research institutions in France or abroad, or from public or private research centers.

L'archive ouverte pluridisciplinaire **HAL**, est destinée au dépôt et à la diffusion de documents scientifiques de niveau recherche, publiés ou non, émanant des établissements d'enseignement et de recherche français ou étrangers, des laboratoires publics ou privés.

Selective manipulation of microscopic particles with swirling Rayleigh waves

Antoine Riaud

*Institut d'Electronique, de Microélectronique et Nanotechnologie (IEMN), LIA LICS,
Université Lille 1 and EC Lille, UMR CNRS 8520, 59652 Villeneuve d'Ascq, France and
CNRS UMR 7588, UPMC Université Paris 06, Institut des NanoSciences de Paris (INSP), F-75005, Paris, France*

Michael Baudoin and Olivier Bou Matar

*Institut d'Electronique, de Microélectronique et Nanotechnologie (IEMN), LIA LICS,
Université Lille 1 and EC Lille, UMR CNRS 8520, 59652 Villeneuve d'Ascq, France*

Loic Becerra and Jean-Louis Thomas

CNRS UMR 7588, UPMC Université Paris 06, Institut des NanoSciences de Paris (INSP), F-75005, Paris, France

(Dated: June 29, 2016)

Acoustical vortices offer tremendous perspective for dexterous contactless manipulation. In order to fulfill their potential of selective though label-free biocompatible tweezers, they must nonetheless become flat, smaller and easily integrable with disposable substrates. In this letter, we synthesize acoustic vortices using an integrated transducer by solving an inverse problem. We then capture and pattern tens of 30 μm particles on disposable substrates. Finally, we compare the forces applied by our vortices to theoretical calculations. This technology offers numerous prospects for micro-fabrication and cell-printing.

High precision contactless manipulation offers tremendous perspectives for biophysical investigations and breakthroughs such as biological cell printing. A large span of methods using magnetic [1, 2], optical [3, 4], electrical [5] and acoustical forces [6, 7], and their combination [8] have been proposed. Among these techniques, acoustic tweezers stand out for cell manipulation applications as they combine high bio-compatibility [9], label-free manipulation [10], relatively low cost and disposable parts for minimized sample contamination [11]. One approach to capture individual particles relies on an ultrasonic beam in the Mie scattering regime (particle size \gg wavelength) [12]. Herein, very high frequencies (between 100 MHz and 1 GHz) are required to achieve selective manipulation, resulting in a deleterious heating of the manipulated sample [13] and the need of high-end electronics.

Alternative technologies based on Rayleigh scattering (particle size \ll wavelength) allow contactless manipulation of micro-objects at much lower frequency (30 MHz). In the first one [14, 15], two orthogonal standing surface acoustic waves (SAWs) create an egg-box potential well network where numerous particles can be captured and translated at once. Standing SAWs traps are flat devices easily miniaturized [16], and benefit from an expeditive fabrication by photolithography. Nonetheless, the simple nature of the acoustic field generated by this kind of device are unsuitable to manipulate selectively one particle within a cluster.

Dexterous and selective contactless manipulation was recently achieved [17–19] using acoustical vortices. These helical waves spin around a phase singularity where wavefront dislocation yields a total cancellation of the beam amplitude. This dark spot is wrapped by a bright ring

of maximum sound intensity which in turn enables a selective trapping at this dark focus [20]. Nevertheless, the synthesis of acoustical vortices is challenging: it requires most often a network of numerous transducers controlled by a high-end programmable electronics. In such configuration, the large number of individual transducers makes the miniaturization challenging and the electronic hardware skyrockets the device cost. Finally, these devices and their successive improvements [21, 22] are not flat which complicates integration with other microfluidic elements.

We recently expanded the surface acoustic wave toolbox with the 2D anisotropic analog of acoustical vortices called swirling SAWs [23]; these waves in turn generate acoustical vortices when immersed in a liquid [24]. Similarly to their 3D analog, the experimental synthesis of swirling SAWs is challenging and so far involves 32 interdigitated transducers (IDT) controlled independently by a high end programmable electronics. In this letter, we synthesize swirling SAWs and acoustical vortices with a single spiraling IDT and a single oscillating voltage source. These spiraling IDTs constitute the core of a new class of swirling SAW acoustic tweezers able to generate acoustical vortices at remote locations through several layers of materials. We quantify the forces applied by the acoustic radiation pressure of these vortices on 30 μm polystyrene (PS) particles. We then use this tweezers to pattern individually several dozens of particles. This technology is selective, label-free, cheap, flat, easy to miniaturize, biocompatible and involves disposable chips. It could finally allow acoustic tweezers to reach standard laboratory workbench and enable a whole range of new biophysical assays and micro-fabrication processes.

Our acoustic tweezer setup (see figure 1) combines a

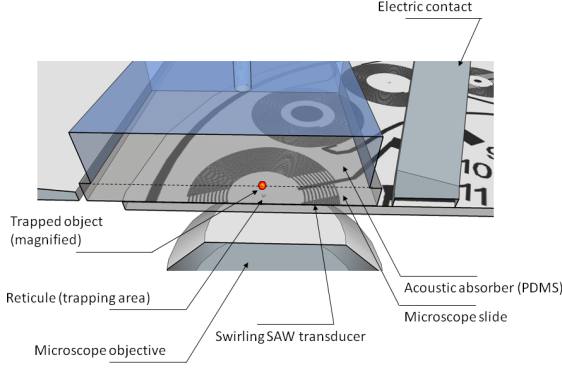


FIG. 1. The transducer is a pair of spiraling interdigitated gold electrodes deposited on a piezoelectric substrate. A microscope slide is placed on the transducer, and acoustic contact is ensured by the mean of a thin layer of silicon oil. An aqueous suspension of micrometric polystyrene beads is dispersed between the microscope slide and an upper layer of PDMS that plays the role of acoustic absorber. The center of the vortex is visualized by a reticule.

static part (the transducer) and a mobile part (the substrate) placed atop of it, sandwiching a very thin matching layer of silicon oil. We displace individual particles by placing the transducer below one of them, turning the power on, moving the transducer and the captured object to the desired place and then turning the power off again. For practical reasons (simpler electrical connections and visualization), the transducer is fixed in the laboratory frame and the sample is mobile by the mean of a micromanipulator.

Surface acoustic waves are nanometric mechanical vibrations of pulsation ω propagating at the surface of a generally anisotropic substrate with a slowness $s_{SAW}(\psi)$ that depends on the direction of propagation ψ . This dispersion relation restricts the variety of fields that can be synthesized. Any surface acoustic wave can therefore be written as follows [23]:

$$\Xi^{(0)} = e^{i\omega(t-\tau)} \int_{-\pi}^{\pi} \mathcal{H}^{(0)}(\psi) e^{-i\omega h(\psi, \theta)r} d\psi, \quad (1)$$

where $\Xi^{(0)}$ is the normal vibration amplitude of the substrate at the point (r, θ) in polar coordinates and at time t . We introduce the convenient notation $h(\psi, \theta) = s_{SAW}(\psi) \cos(\psi - \theta)$. In equation (1), $\mathcal{H}^{(0)}$ is the angular spectrum of the wave, that is the relative weight of the plane waves for each direction ψ . The angular spectrum is the sole degree of freedom in equation (1). For subsequent discussion, we introduce the complex phase μ and amplitude ξ of $\mathcal{H}^{(0)}(\psi) = \xi(\psi)e^{i\mu(\psi)}$ and a delay τ .

At the surface of piezoelectric materials, surface acoustic waves combine periodical displacements in the three

directions of space and electrical oscillations, the proportion of each of them being ψ -dependent. In the following, we will refer to $a(\psi)$ as the normal substrate vibration amplitude per unit voltage. (a and s_{SAW} are provided in the supplemental material). Reversely, this fundamental electromechanical coupling ensures that forcing an alternative current through a piezoelectric substrate provokes periodical deformations of the solid. IDTs are a special pattern of electrodes that reinforce these vibrations by constructive interferences. Here, an alternate grating of hot and ground electrodes with the same spatial period as the wave generates a surface wave when it vibrates in phase with the SAW. It is nonetheless challenging to fulfill these resonance conditions due to the substrate anisotropy, which restricts interdigitated transducers to plane waves and in very few cases to focused waves. Consequently, although swirling SAWs have been experimentally synthesized, no mathematical background is currently available to design a suitable integrated transducer for these waves.

In the supplemental material, we conceive an integrated transducer suitable to generate an arbitrary SAW field $\Xi^{(0)}$. In our calculations, the hot and ground electrodes run along a polar curve $R(\Omega)$ and are exposed to an alternative tension $V(\Omega)$:

$$V(\Omega) = e^{i\omega t} \frac{\xi(\bar{\psi} + \pi)\sqrt{2\pi}}{|a(\bar{\psi})|\sqrt{R(\Omega)\omega|h''(\bar{\psi}, \Omega)|}}, \quad (2)$$

$$R(\Omega) = \frac{\psi_0 + \alpha(\bar{\psi}) - \frac{\pi}{4} \text{sgn}(h''(\bar{\psi}, \Omega)) - \mu(\bar{\psi} + \pi)}{\omega h(\bar{\psi}, \Omega)}, \quad (3)$$

where ψ_0 is a free parameter: $\psi_0 = \omega\tau + b\pi$ for the hot electrode and $\psi_0 = \omega\tau + (b+1)\pi$ for the ground, with $b \in \mathbb{Z}$ a dummy parameter introduced for symmetry reasons (see the derivation of equations (2) and (3) in the supplemental material). $\alpha(\bar{\psi})$ is the complex argument of $a(\bar{\psi})$. In this equation, the beam stirring angle $\Omega - \bar{\psi}(\Omega)$ is defined by $h'(\bar{\psi}) = 0$ with $h' = \frac{\partial h}{\partial \bar{\psi}}$. As pointed out by Laude et al [25], $h(\bar{\psi}, \Omega)$ is related to the group velocity $v_g(\Omega) = 1/h(\bar{\psi}, \Omega)$. The term $\sqrt{|h''(\bar{\psi}, \Omega)|}$, proportional to the phonon focusing factor, may vanish for some material cuts in some directions, in which case it yields cuspidal points and caustics. In equations (2) and (3) the offset of π of μ and ξ arguments represents the fact that the electrode located at Ω generates a plane wave propagating with a direction $\bar{\psi}(\Omega) + \pi$. The term \sqrt{R} accounts for the antenna gain of the transducer.

Although R is fairly easy to calculate and tune, V —the excitation magnitude of a specific IDT portion—mostly depends on $a(\psi)$ which is specific to the material and its cut (see also [26]). Setting V may involve the ability to apply different voltage magnitudes on different finger pairs or increasing the number of finger pairs in the directions of weaker coupling $a(\bar{\psi})$.

An exciting application of this inverse problem is the synthesis of acoustic vortices, which may in turn achieve selective contactless manipulation of microparticles and biological cells. According to earlier studies [23], the acoustic field radiated by anisotropic substrates can only generate anisotropic swirling SAWs (as opposed to usual Bessel beams):

$$\mathcal{W}_l = \frac{e^{i\omega t}}{2\pi i^l} \int_{-\pi}^{\pi} \rho(\psi) e^{il\psi - ih(\psi, \theta)r} d\psi, \quad (4)$$

where l is the topological charge of the vortex, and $\rho(\psi)$ is a free parameter to give some flexibility for later discussion.

It was also shown that anisotropic waves are prone to degeneration when traveling through isotropic media [24]. This degeneration can be controlled by synthesizing adequate precursor waves of angular spectrum $\mathcal{H}^{(0)}$ on the substrate that degenerate into the desired field of angular spectrum $\mathcal{H}^{(n)}$ after crossing n superstrates. According to the angular spectrum propagation calculations in supplemental material, we get:

$$\mathcal{H}^{(0)} = \mathcal{H}^{(n)} e^{i\omega\mathcal{T}}, \quad (5)$$

$$\mathcal{T} = \sum_{i=1}^n s_z^{(i)} (z_i - z_{i-1}), \quad (6)$$

$$s_z^{(i)} = \sqrt{s^{(i)^2 - s_{SAW}^2}, \quad (7)$$

with, in the case of acoustical vortices,

$$\mathcal{H}^{(n)} = \frac{\rho(\psi) e^{il\psi}}{2\pi i^l}. \quad (8)$$

$e^{i\omega\mathcal{T}}$ is the propagator, where \mathcal{T} represents the direction-dependent delay due to the propagation across n superstrates of slowness $s^{(i)}$, $i \in \{1..n\}$ with their interface located at z_i . In order to create the acoustic vortex given by equation (4), we generate the precursor wave which angular spectrum is given by equation (5) and (8). This wave is in turn synthesized by the transducer described by equation (3). Those calculations are implemented in the Python code in supplemental material.

Importantly, equations (3) and (5) show that R depends on the frequency of actuation, the slowness of the piezoelectric substrate and the superstrates, and on the thickness of each superstrate layer. Accordingly, each transducer has to be designed specifically for this set of parameters. This is not very restrictive since standardized microscope slides and coverslips made of glass and other materials are readily available.

Remarkably, the final geometry of the transducer seems suitable for super-harmonic generation. Accordingly, harmonic m is expected to generate an acoustic vortex of charge lm when excited at a pulsation $\omega_m = m\omega$ (proof in the supplemental material).

In a first set of experiments, we fabricated the transducer shown in figure 2.A to form acoustical vortices \mathcal{W}_1

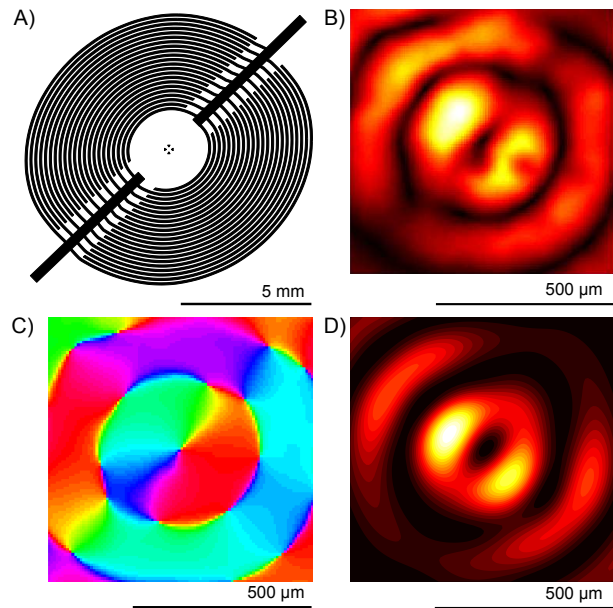


FIG. 2. **A)** Spiraling swirling SAW transducer (\mathcal{W}_1 at 10 MHz across #1 glass coverslip), **B)** Experimental substrate vertical vibrations amplitude (max amplitude 1.4 nm_{pp} at 7 V_{rms}), **C)** Experimental substrate vertical vibrations phase, **D)** Calculated potential well from experimental data (max height 6.3 fJ)

across a typical glass coverslip (#1 borosilicate, thickness 200 μm). The lithography process and the masks are available in supplemental material. The transducer twists hot and ground electrode in a double Archimedes spiral. The diameter of the device is constrained by the attenuation of the leaky surface wave, approximately 2 dB/MHz/cm. The hot and ground electrodes are connected on opposite supply branches, the branches themselves being located in the minimal piezoelectric coupling directions. The working frequency of this specific device is 10 MHz, which corresponds to wavelengths near 400 μm and optimal object size close to 70 μm [16, 17]. Standard lithography workbench allows resolutions up to 1 μm , which lets envision the manipulation of sub-micrometric object with a similar setup.

In order to measure the vertical vibrations created by this transducer, we coated a glass coverslip with a thin layer of gold. We then measured the vertical vibration amplitude of the substrate (see figure 2.B and C) using a home-made vibrometer described previously [23]. The experiment is as follows: we drop a small volume of silicon oil (1.0 Pa.s) directly on the transducer surface and then squeeze the liquid with a gold-coated coverslip. Finally, we add a small droplet of water and cap it with a millimeter thick block of cross-linked polydimethylsiloxane (PDMS) to minimize acoustic reflections. The Michelson vibrometer then measures the vibrations of the top surface of the coverslip. Accordingly, the vortex diameter sizes roughly $\lambda/2 = 175 \mu\text{m}$. The phase singu-

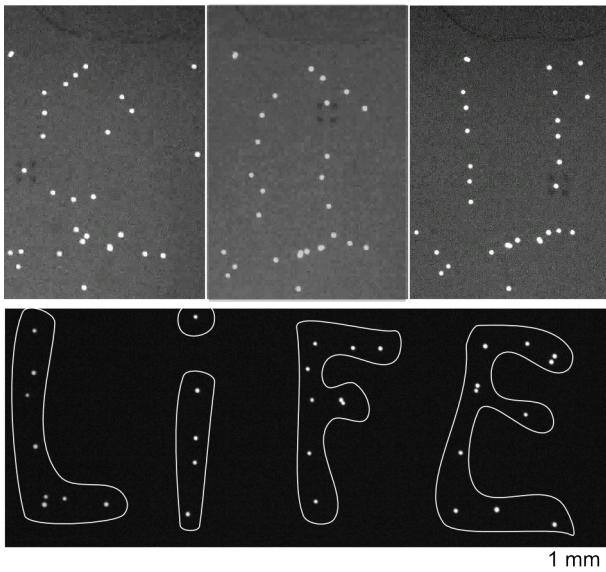


FIG. 3. Manipulation of 30 μm PS beads. Top: rearrangement of a random distribution of beads into of two vertical lines. Bottom: writing of the word LIFE with 33 particles.

larity shown in figure 2.C is clearly visible and validates the calculation of R . It results directly in the dark core in the center of figure 2.B. Knowing the vertical vibration amplitude (about $1.4 \text{ nm}_{\text{pp}}$ at $7 V_{\text{rms}}$), it is possible to compute the force applied by this vortex on spheres. In the case of small particles, this force is the gradient of the potential [27] shown in figure 2.D. The theoretical calculation and maximum displacement speed experiments (details in supplemental material) agree quantitatively well on a maximum force of 200 pN on 30 μm PS spheres at $7 V_{\text{rms}}$, which is also the upper bound of optical tweezers [4].

We then used a similar transducer to arrange sets of dozens of 30 μm PS spheres. The rearrangements took a few minutes and is shown in figure 3. It happens by iteratively grabbing, moving and dropping individual beads as mentioned earlier (see video in supplemental material).

These rearrangement experiments may be perturbed by the secondary basin of attraction on the edge of the vortex which can also capture individual beads. Thus, a competition between the acoustic radiation pressure of the vortex at the core and the secondary rings, and the friction due to the fluid and the solid will decide which beads stay in place and which ones move with the vortex. Therefore, the selectivity of the device comes from the larger force at the center of the vortex than on the secondary rings which allows choosing a friction threshold in between. Since PS beads showed little friction with glass, we switched to poly(methyl methacrylate) (PMMA) coverslips with a thickness of 2.0 mm and modified the transducer accordingly (mask in supplemental material).

The iterative process to form two lines of particles on this PMMA superstrate is shown at the top of figure 3, and the final arrangement of 33 beads to form the word LIFE is shown at the bottom of figure 3. We believe such rearrangement is figurative of future biological and other microstructures sequential assembly where numerous different cells or particles could be arranged in space.

In this paper, we solved an inverse problem to design integrated transducers for arbitrary acoustic fields. We then applied this solution to design an integrated spiraling transducer for acoustic vortices. The resulting acoustic field efficiently captures individual micrometric particles with forces up to 200 pN. The insertion of a micromanipulator to force a relative motion between the transducer and the container of the beads allows selective rearrangements of dozens of microspheres. This research opens exciting prospects for cell printing and tissue engineering where dozens of different cell types could be combined and placed accurately to study or print complex biological tissues.

The authors gratefully acknowledge the PMCLAB for their support in fabricating the micromanipulation interface. This research was funded by ANR-12-BS09-0021-01/02 and Région Nord Pas de Calais.

-
- [1] I. De Vlaminck and C. Dekker, Annual review of biophysics **41**, 453 (2012).
 - [2] F. Martinez-Pedrero and P. Tierno, Physical Review Applied **3**, 051003 (2015).
 - [3] A. Ashkin, J. Dziedzic, J. Bjorkholm, and S. Chu, Optics letters **11**, 288 (1986).
 - [4] J. R. Moffitt, Y. R. Chemla, S. B. Smith, and C. Bustamante, Biochemistry **77**, 205 (2008).
 - [5] J. Voldman, Annu. Rev. Biomed. Eng. **8**, 425 (2006).
 - [6] R. Moroney, R. White, and R. Howe, Applied physics letters **59**, 774 (1991).
 - [7] J. Shi, D. Ahmed, X. Mao, S.-C. S. Lin, A. Lawit, and T. J. Huang, Lab on a Chip **9**, 2890 (2009).
 - [8] P. Y. Chiou, A. T. Ohta, and M. C. Wu, Nature **436**, 370 (2005).
 - [9] M. Wiklund, Lab on a Chip **12**, 2018 (2012).
 - [10] X. Ding, Z. Peng, S.-C. S. Lin, M. Geri, S. Li, P. Li, Y. Chen, M. Dao, S. Suresh, and T. J. Huang, Proceedings of the National Academy of Sciences **111**, 12992 (2014).
 - [11] F. Guo, Y. Xie, S. Li, J. Lata, L. Ren, Z. Mao, B. Ren, M. Wu, A. Ozelik, and T. J. Huang, Lab on a Chip **15**, 4517 (2015).
 - [12] J. Lee, S.-Y. Teh, A. Lee, H. H. Kim, C. Lee, and K. K. Shung, Applied physics letters **95**, 073701 (2009).
 - [13] V. Marx, Nature methods **12**, 41 (2015).
 - [14] S. Tran, P. Marmottant, and P. Thibault, Applied Physics Letters **101**, 114103 (2012).
 - [15] X. Ding, S.-C. S. Lin, B. Kiraly, H. Yue, S. Li, I.-K. Chiang, J. Shi, S. J. Benkovic, and T. J. Huang, Proceedings of the National Academy of Sciences **109**, 11105 (2012).
 - [16] D. J. Collins, B. Morahan, J. Garcia-Bustos, C. Doerig,

- M. Plebanski, and A. Neild, *Nature communications* **6** (2015).
- [17] D. Baresch, J.-L. Thomas, and R. Marchiano, *Physical Review Letters* **116**, 024301 (2016).
- [18] A. Marzo, S. A. Seah, B. W. Drinkwater, D. R. Sahoo, B. Long, and S. Subramanian, *Nature communications* **6** (2015).
- [19] C. R. Courtney, C. E. Demore, H. Wu, A. Grinenko, P. D. Wilcox, S. Cochran, and B. W. Drinkwater, *Applied Physics Letters* **104**, 154103 (2014).
- [20] P. L. Marston, *The Journal of the Acoustical Society of America* **120**, 3518 (2006).
- [21] N. Jiménez, R. Picó, V. Sánchez-Morcillo, V. Romero-García, L. M. García-Raffi, and K. Staliunas, arXiv preprint arXiv:1604.08353 (2016).
- [22] C. J. Naify, C. A. Rohde, T. P. Martin, M. Nicholas, M. D. Guild, and G. J. Orris, arXiv preprint arXiv:1604.08447 (2016).
- [23] A. Riaud, J.-L. Thomas, E. Charron, A. Bussonnière, O. B. Matar, and M. Baudoin, *Physical Review Applied* **4**, 034004 (2015).
- [24] A. Riaud, J.-L. Thomas, M. Baudoin, and O. B. Matar, *Physical Review E* **92**, 063201 (2015).
- [25] V. Laude, D. Gerard, N. Khelifaoui, C. F. Jerez-Hanckes, S. Benchabane, and A. Khelif, *Appl. Phys. Lett.* **92**, 094104 (2008).
- [26] V. Laude, C. Jerez-Hanckes, and S. Ballandras, *IEEE Trans. Ultrason., Ferroelectr., Freq. Control* **53**, 420 (2006).
- [27] L. Gor'Kov, in *Soviet Physics Doklady*, Vol. 6 (1962) p. 773.